Asian Journal of Chemistry Vol. 21, No. 6 (2009), 4617-4627

Enhanced Performance of Nano γ-MnO_2/Mesocarbon Microbeads Composite as Electrocatalyst for Solid State Zinc-Air Cells

SHENG-TAO ZHANG* and GUO-QING ZHANG†
College of Chemistry and Chemical Engineering, Chongqing University, Chongqing-400030, People's Republic of China
Fax: (86)(23)72790008; Tel: (86)(23)72790008
E-mail: yzhanggq@163.com

Nanostructured γ-MnO_2/MCMB (mesocarbon microbeads) composite has been prepared as electrocatalyst for application in solid-state zinc-air cell. Scan electronic microscopy and X-ray diffraction show that the MnO_2 uniformly covers on the surface of MCMB with the typical γ-MnO_2 composition. The electrocatalytic activity of the composite for oxygen electrode was examined by cathode polarization curve, chronoamperometry and electrochemical impedance spectroscopy (EIS). Results indicate that the electrocatalytic activity for oxygen reduction of the composite is better than that of single γ-MnO_2. All solid-state zinc-air cell fabricated using this electrocatalyst exhibits good discharge performance. An energy density of 320 wh kg^{-1} was obtained with a power density of 27.4 w kg^{-1} at discharge current of 10 mA cm^{-2}. The γ-MnO_2/MCMB composite has potential application in zinc-air cells.

Key Words: Nano-structures, Zinc-air cell, Electrocatalyst, Oxygen reduction reaction.

INTRODUCTION

Zinc-air battery, possessing many advantages such as a higher specific energy, *i.e.*, more than 200 Wh kg^{-1} compared with other zinc-based alkaline batteries, a much flatter working voltage, a higher capacity density, which is independent of load and temperature, has been focused in the past years[1-7]. Gas diffusion oxygen electrode (*i.e.* air cathode), where molecular oxygen is electrocatalytically reduced is vital to zinc-air battery. The power output of zinc air cells is mainly limited by the high polarization of air cathode that is ascribed to a slow catalytic reduction of oxygen. Air cathode used in zinc air cells is designed to optimize contact between reactant and electrolyte to maximize reaction rate. Catalysts are commonly incorporated into air cathode structure to increase the rate of oxygen reduction. There have been many attempts over the past years to find inexpensive highly active catalysts and a process for making them. Noble metals such as platinum as electrocatalyst for molecular oxygen reduction in gas diffusion oxygen electrode are well known.

†Department of Chemistry and Environment Science, Yangtze Normal University, Fuling-408100, People's Republic of China.

They offer the advantages of high catalytic activity, electronic conductivity and stability, their high costs and susceptibility to catalyst poisoning are a serious concern for commercial applications. As one of promising pathway to replace platinum, manganese oxide as electrocatalyst for oxygen reduction has been long-time investigated[8-13]. It has been discovered that manganese oxide can be act as a suitable catalyst for air cathode. As an electrocatalyst for oxygen electroreduction, catalytic activity of manganese oxide is closely related to its electrochemical activity[12]. Among various types of manganese oxides, an electrochemically active form is γ-MnO_2, which has been commercially used as cathode material in alkaline batteries. So, γ-MnO_2 is the most favourable form of manganese oxide for oxygen electroreduction.

Brenet[14] proposed that the electrochemical reduction of molecular oxygen occured through reduction and oxidation of the redox couple Mn^{4+}/Mn^{3+}. Matsuki and Kamada[15] also examined the oxygen reduction reaction on some crystalline manganese oxides in alkaline solutions using a rotating ring-disk electrode and Teflon-bonded electrode. They suggested that manganese oxides with much more active sites increased its electrocatalytic activity for the oxygen reduction reaction. Because the electrocatalytic process for oxygen reduction involves the reduction and oxidation of surface manganese ions, the number and activity of the redox centers would be important factors for the electrocatalytic performance.

Since Honda and Yamada[16] first separated spheres from the mesophase pitches naming mesocarbon microbeads (MCMB), this material has been used as the precursor for high performance carbon material, such as high density carbon material[17,18], filler for high-performance liquid chromatography[19], active carbon with super-high surface[20] and anode of lithium ion battery[21-25]. To the best of our knowledge, all solid state zinc-air cell by using γ-MnO_2/MCMB as electrocatalyst has yet not been reported. In present work, we reported nanostructured γ-MnO_2 coating on the surface of MCMB as an electrocatalyst for the oxygen reduction reaction and examined its electrocatalytic performance in solid state zinc-air primary cells.

In the fabrication of solid state zinc-air cell, an alkaline polymer gel electrolyte based on potassium salt of cross-linked poly (acrylic acid) was used. This alkaline polymer electrolyte is attractive due to its capability to store much more KOH solution[26], which leads to very high ionic conductivity. At the same time, as an electrolyte, it can avoid rapid evaporation of water from the gel.

EXPERIMENTAL

Synthesis of electrocatalyst: γ-MnO_2 was synthesized by following route. A solution was prepared firstly by adding 12 g of $MnSO_4 \cdot H_2O$ (A.R) to 180 mL distilled water. According to chemical stoichiometric ratio, 16.9 g $Na_2S_2O_8$ (A.R) was added to the prepared solution, stirred and then refluxed 18 h at 50 °C, 3 h at 75 °C, 1 h at 85 °C and 0.5 h at 100 °C. Until the reaction was completed, pH decreased to less than 0.5. After the suspension cooled to room temperature, it was filtered and washed with several portions of distilled water until the filtered solution was neutrality. The obtained solid was dried at 100 °C for 8 h in an oven.

γ-MnO_2/MCMB composite was synthesized as the same route. Mesocarbon microbeads (MCMB) was provided by Shanshan Science and Technology Corp (Shanghai). 1.54 g of MCMB (specific area = 3.5 m^2 g^{-1}) and 12 g $MnSO_4 \cdot H_2O$ (AR) were added into 180 mL distilled water to prepare a suspension. According to chemical stoichiometric ratio, 16.9 g $Na_2S_2O_8$ (A.R) was added to the solution, stirred and then refluxed. The other process was the same as preparing γ-MnO_2. The resulted composite consisted of γ-MnO_2 coating on the surface of MCMB with weight ratio of 4:1.

Preparation of electrode: In fabrication of air electrode, one layer gas diffusion electrode was made. γ-MnO_2/MCMB was used as electrocatalyst and Na_2SO_4 (AR) as pore-forming filler. A mixture containing γ-MnO_2/MCMB, acetylene black (AB), Na_2SO_4 and polytetrafluoroethylene (PTFE, from Aldrich) with weight ratios of 5:1:4:1 was mixed and ground in excess ethanol. Then the mixture was placed onto a porous nickel substrate followed by roll-pressing it at 3 × 107 kg cm^{-2} for 5 min to prepare cathode sheet. The cathode sheet was controlled at 1~4 mm of thickness and cut into a circular shape (14 mm diameter) to prepare air cathode plate. As a comparison, γ-MnO_2 was also used as electrocatalyst to prepare air electrode with the same method described above.

Compacted zinc electrode was made of Zn powder (Toho Zinc Co. Ltd, Japan) and PTFE binder. The mixture containing 0.5 g zinc powder and 60 % PTFE solution was placed onto a circular nickel substrate mesh (14 mm diameter) followed by pressing it at 3 × 107 kg cm^{-2} for 5 min to prepare anode plate.

Cell assembly: All solid state zinc-air cell assembly is the same as literature[27]. All components were enclosed in a cylindrical plastic casing of dimensions: 20 mm (height), 14 mm (diameter). Both ends were attached with screwed, L-shaped, plastic rings. The electrodes were placed on to the L-shaped rings. First, ring with the air cathode was attached to the container. The gel electrolyte was then introduced. Finally, the container was encapsulated with the zinc anode ring.

Structure characterization of the γ-MnO_2/MCMB was performed by means of X-ray diffractometer (MAC M18XCE) with CuKα radiation. Morphology was investigated with scanning electron microscope (SEM) (Leo-1430VP). Polarization character-istic of the oxygen electrodes was carried out by CHI 660A electrochemical workstation (CH Instrument, Cordova TN). Measurements were performed in a typical three-electrode cell with the air electrode as the working electrode, Hg/HgO electrode as the reference electrode and a platinum foil as the counter electrode. The prepared alkaline polymer gel electrolyte was used as electrolyte. Electrochemical impedance spectroscopy and equivalent circuit investigation of air-electrode was performed by means of Autolab Modular Electrochemical Instruments (Autolab/PGSTAT30). Fabricated zinc-air cells were characterized with galvanostatic charge-discharge unit (Arbins AT2042, U.S.). Discharge currents applied were 15.37 mA (10 mA cm^{-2}), 30.74 mA (20 mA cm^{-2}) and 76.85 mA (50 mA cm^{-2}).

RESULTS AND DISCUSSION

XRD analysis: X-ray diffraction pattern of γ-MnO_2/MCMB is shown in Fig. 1. The pattern indicates well-defined reflection, which means crystalline structure. The diffractive peaks of γ-MnO_2/MCMB were assigned as 22.45º (120), 34.49º (031), 37.15º (131), 38.81º (230), 42.64º (300), 56.19º (160), 62.50º (401), 65.65º (421) and 68.94º (003) (JCPDF-14-0644) except 26.4º (002) that is attributed to that of MCMB. Structural analysis further reveals that MnO_2 is composed of typical hexagonal γ-MnO_2, which has lattice parameters of a = 6.36 Å, b =10.15 Å, c = 4.09 Å. This kind of manganese oxide is widely considered as the most electrochemical active material for battery. The electrocatalytic activity of manganese oxide for oxygen reduction is closely related to the electrochemical activity, therefore it is predicted that this composite would be outstanding electrocatalyst for oxygen reduction reaction.

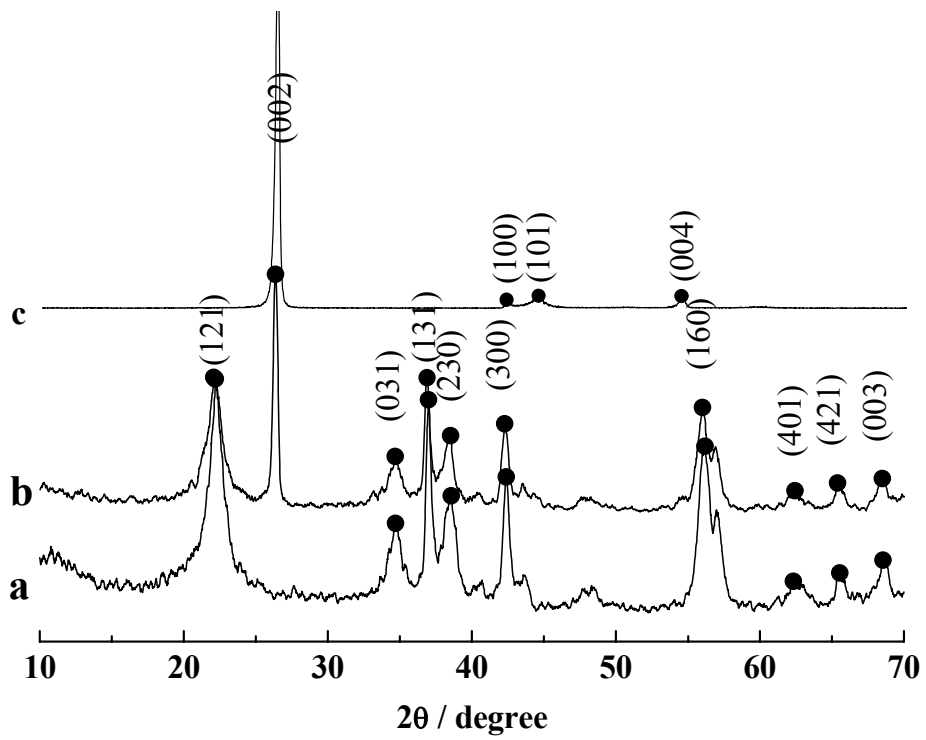

Fig. 1. XRD patterns of γ-MnO_2 (a), γ-MnO_2/MCMB (b) and MCMB (c)

Morphology analysis: It would be interesting to examine the morphology of the material, which has been in the form of powders. From SEM images presented in Fig. 2, at a low magnification, both γ-MnO_2 and γ-MnO_2/MCMB tend to form irregular spherical particles having rod-like protrusions from each particle surface. Average spherical particle size is around 2-40 μm. At a high magnification of 100,000,

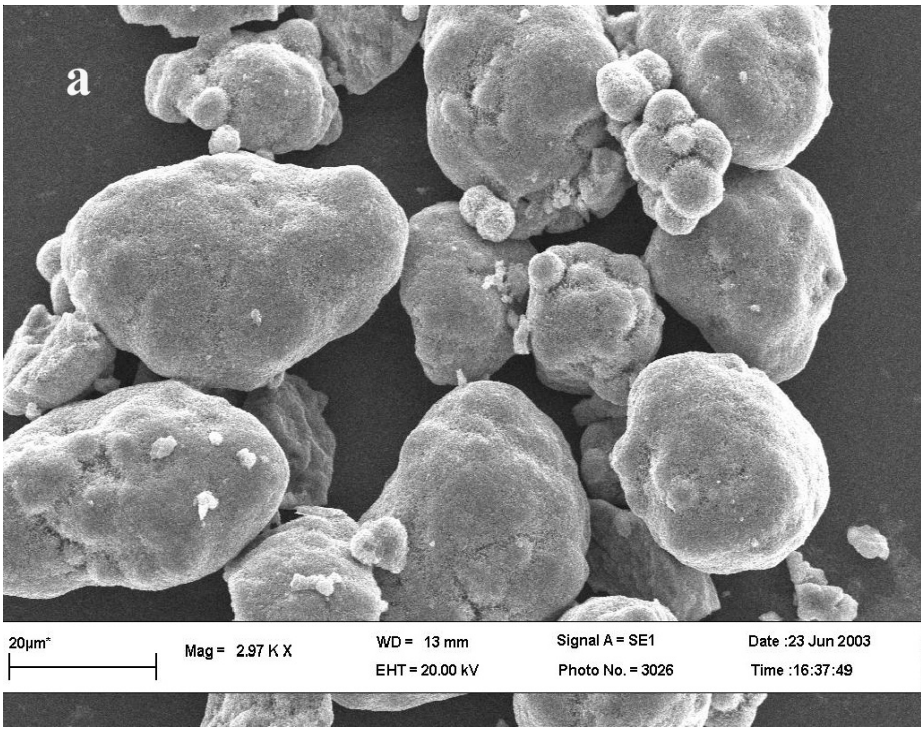
a
20µm*
Mag = 2.97 K X
WD = 13 mm
EHT = 20.00 kV
Signal A = SE1
Photo No. = 3026
Date :23 Jun 2003
Time :16:37:49

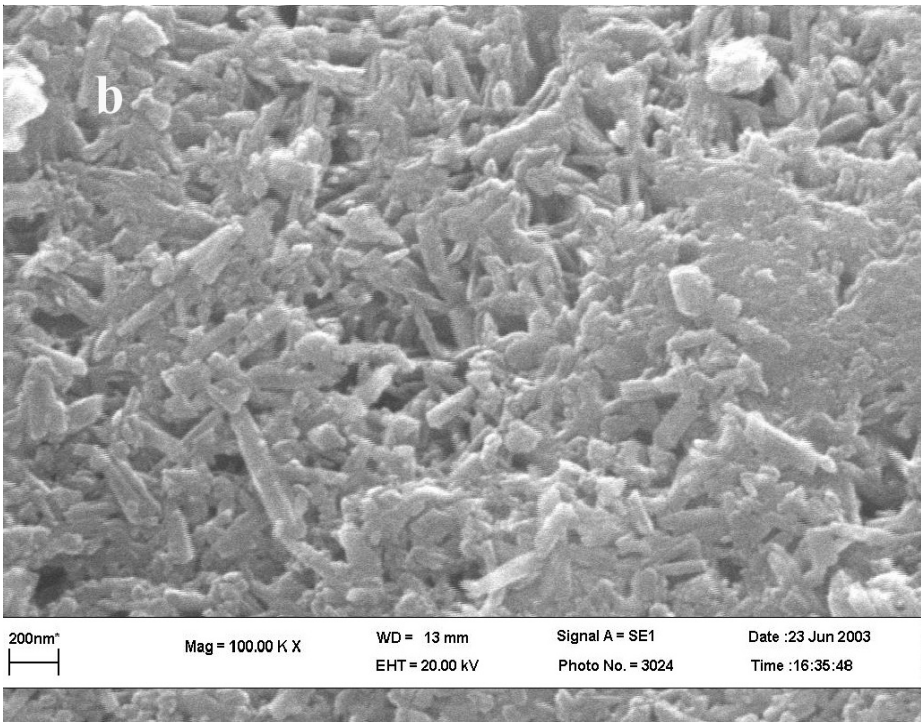
b
200nm*
Mag = 100.00 K X
WD = 13 mm
EHT = 20.00 kV
Signal A = SE1
Photo No. = 3024
Date :23 Jun 2003
Time :16:35:48

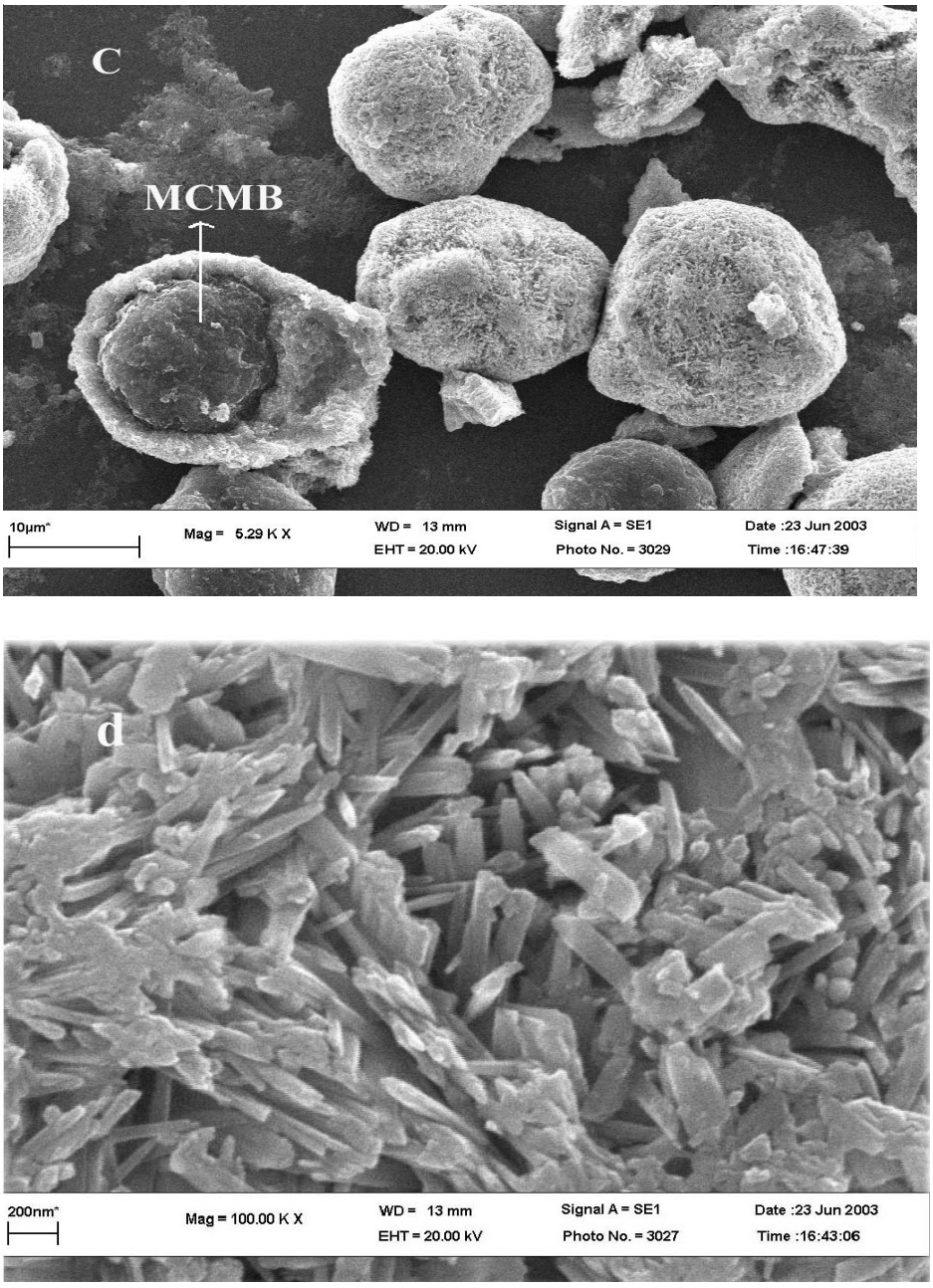

Fig. 2. SEM images of γ-MnO_2 (a, b) and γ-MnO_2/MCMB (c, d)

SEM of the γ-MnO_2/MCMB shows the existence of bird's nest morphologies and rod-like protrusions. The composite is actually made up of solid rods of γ-MnO_2 with about 200 nm length and nanoscale pores between rods coating on the surface

of MCMB. Rod-like γ-MnO_2 protrusions and small pore size offer the material with high surface area and more available space to electrolyte. This morphology might be favourable for oxygen reduction reaction. Especially, MCMB acting as electrocatalyst support would be sharply increased the conductivity of the material. It is important to design a gas diffusion electrode that electrolyte can penetrate into but not over-flood and that the electrode has good conductivity. In the gas diffusion oxygen electrode, increasing of electrocatalyst conductivity would be decrease the over-potential of the oxygen reduction reaction. Special morphology like that of the γ-MnO_2/MCMB would provide much convenience to the electrode design. The pores of the composite can provide channels for the electrolyte and air moving into the catalyst, which can increase the gas-liquid interfacial area and give much more opportunity for oxygen dissolution and diffusion. Also, the presence of these nanostructured γ-MnO_2 protrusions resulted in materials having a high density of active sites for promoting fluid/solid reactions and pores between γ-MnO_2 provide a relatively easy path for percolation of the reactive fluid or gas through composite. The short diffusion distance into and out of the chemically or catalytically active agglomerates ensures a high reaction rate[28]. In addition, due to the submicron radius of these pores, the capillary force would be strong enough to hold the electrolyte and prevent it from over flooding the electrode. Thus the gas can reach the catalytic sites on the internal surface of γ-MnO_2/MCMB while the electrolyte partially fills the channels.

Polarization characteristics: The polarization curves for oxygen electrodes are shown in Fig. 3. The cathode current for the γ-MnO_2 catalyzed electrode starts to emerge at about -0.1 V and increases slowly as the potential becoming more negative. Whereas the cathode current for the γ-MnO_2/MCMB catalyzed electrode starts at about -0.01 V and increases rapidly. During tests, the cathode current of later is always higher than that of the former electrode. This difference can be attributed to catalytic properties of electrocatalysts used. γ-MnO_2/MCMB has γ-MnO_2 protrusions and more pores between rod-like γ-MnO_2 and the increased conductivity attributed to using MCMB as electrocatalyst support. This is in good agreement with the large current observed for the oxygen electrode catalyzed by γ-MnO_2/MCMB.

Chronnamperometry curve of γ-MnO_2/MCMB-catalyzed air electrode is shown in Fig. 4. The chronoamperometery technique consists of applying a potential jump on the electrode from rest potential to a negative potential and recording the transient current. It is seen from the figure that the cathode currents of air electrode under -0.2, -0.3 and -0.4 V are all increased sharply within short time and then achieve to a relatively stable value. These series of curves show that the cathode current at various potential jumps has an increasing tendency. This characteristic indicates that the air electrode using γ-MnO_2/MCMB can sustain high current discharge.

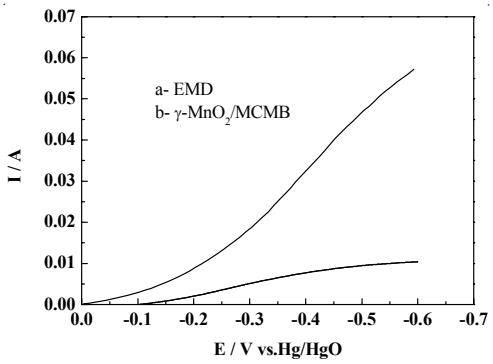

Fig. 3 Cathode polarization curves for oxygen reduction on gas diffusion electrode (a) γ-MnO_2-catalyzed (b) γ-MnO_2/MCMB-catalyzed, scan rate: 5 mV·s^{-1}

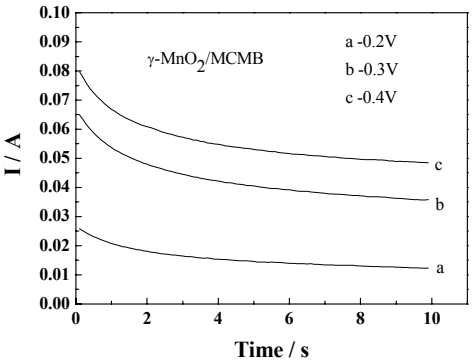

Fig. 4. Chronnamperogram for air electrode using γ-MnO_2/MCMB

Galvanostatic discharge: Discharge profiles at various constant currents are given in Fig. 5. During discharge, zinc at the anode is consumed by conversion to zinc oxide and at the cathode, oxygen from the air is electrochemically reduced to hydroxide ions. It can be seen from Fig. 5 that the cells are able to sustain the current drains, as demonstrated by the flat discharge curves. The open circuit potential all reaches about 1.4 V. At current drain of 15.37, 30.74 and 76.85 mA for the cells with γ-MnO_2/MCMB electrocatalyst, the average voltage plateaus are about 1.07, 0.78 and 0.6 V and discharge last 11.7, 2.8 and 0.34 h, respectively. It is clear that the discharge time of the cells with different electrocatalysts is prolonged significantly at low discharge current. The average working voltage of the cells with γ-MnO_2/MCMB is also promoted about 80-100 mV. From the changes of the discharge time for the zinc-air cells with the different electrocatalysts, it was found that the the catalytic activity of γ-MnO_2/MCMB is higher than that of γ-MnO_2.

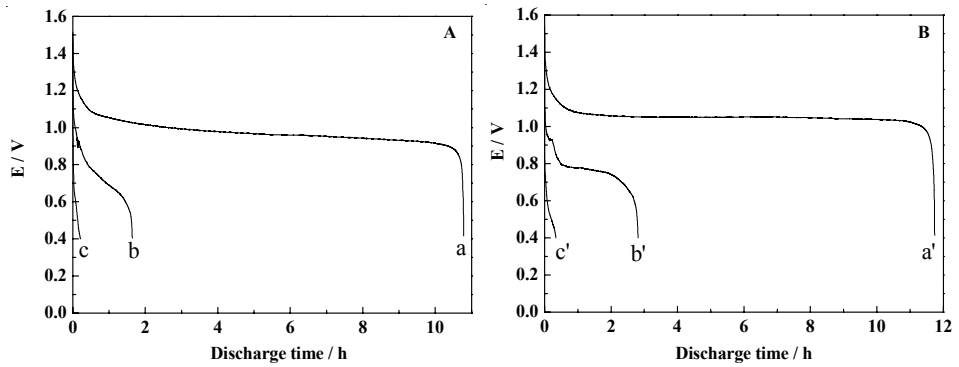

Fig. 5. Typical discharge curves of the zinc-air cells with γ-MnO_2 (a, b, c) and γ-MnO_2/MCMB (a', b', c') as electrocatalyst at different discharge currents (a, a') 15.37 mA; (b, b') 30.74 mA; (c, c') 76.85 mA

The energy density and power density of a cell can be calculated by using the following equations:

$$E = C_m \times \Delta V \quad (1)$$

$$C_m = \frac{I \times t}{m} \quad (2)$$

$$p = \frac{E}{t} = \frac{I \times \Delta V}{m} \quad (3)$$

where C_m is the special capacity of the cell, ΔV, I and t is the operating voltage, discharge current and time; m is the mass summation of positive and negative electrode. By calculation, an energy density of 320 wh kg^{-1} and a power density of 27.4 w kg^{-1} was obtained at discharge current of 10 mA cm^{-2} for the zinc-air cell using γ-MnO_2/MCMB.

EIS Analysis: Typical electrochemical impedance spectra for air electrodes are shown in Fig. 6, in which Nyquist and Bode plot are also presented. The x axis and y axis represent the real part of the impedance (Z′) and the imaginary part of the impedance (Z″). In general, the measured impedance spectra are depressed semicircles in the complex plane and they do not show the "semicircle centered on the real axis" feature that is typically observed in systems that can be represented by a simple resistance-capacitance (RQ) equivalent circuit. The origin of the deviation can be ascribed to the presence of inhomogeneous and porosity upon the electrode surface, which gives rise to a frequency-dependent penetration depth for the ac wave. From the Nyquist impedance spectra, two different sizes of semicircles between the measuring frequencies can be observed. At a high frequency (f >1 kHz), besides the existence of induction, the Nyquist plot is composed of a small-depressed semicircle and Bode plot has a wave peak indicating the presence of reactant, which is attributed to the ohm polarization of the air electrode. At the intermediate frequency (10 Hz < f < 1 kHz), the semicircle is caused by the electrochemical polarization of the air electrode. It can also be seen from the Nyquist plot that at low frequency (f < 10 Hz), the plot has a tendency to change to a straight line that has an angle of 45 ºC. This straight line is a characteristic of the semi-finite diffusion (Warburg impedance Zw). The electrolyte resistance is determined by the point of intersection of the high-frequency semicircle with the real axis.

The fitted circuit is shown in Fig. 7. It can be seen from the Fig. 6 that the Fig. 7 represents the structure of the measured system and some actually kinetic parameters, in which, L is inductance, R_1 is the electrolyte resistance between electrode surface and reference electrode, R_2 represents the surface contact resistance between electrode and electrolyte addition to ohm resistance of air electrode, here, Q_1 and Q_2 represent constant phase element caused by electrode roughness or by inhomogeneous reaction rates on electrode surface, R_3 describes electrochemical polarization resistance, Z_w is Warburg impedance. The calculated kinetic parameters for air electrodes are given in Table-1. From this table, it is evident that the difference of electrolyte

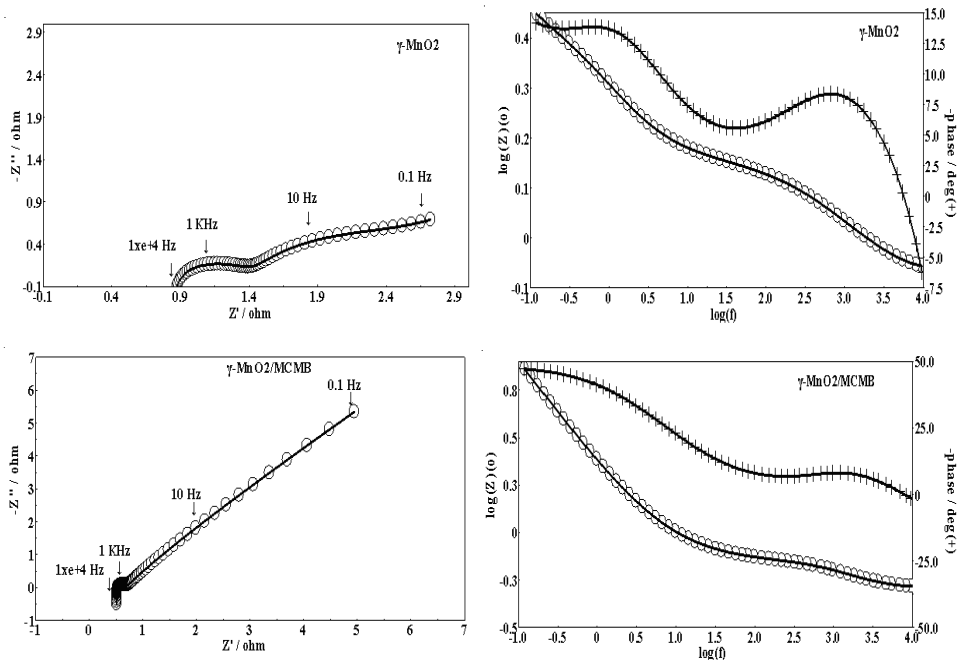

Fig. 6. EIS spectra for air electrodes using γ-MnO_2 and γ-MnO_2/MCMB

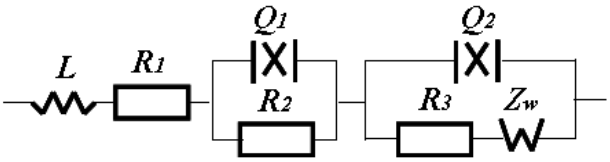

Fig. 7. Equivalent circuit of air electrode for EIS analysis

TABLE-1
ELECTRODE KINETIC PARAMETERS MODIFIED BY EQUIVALENT SIMULATION

Air electrode	L(H)	$R_1(\Omega)$	$R_2(\Omega)$	Q_1 Y_0, n	Q_2 Y_0, n	$R_3(\Omega)$	$W(\Omega)$
γ-MnO_2-catalyzed	0.2688e-5	0.803	0.637	0.5068e-3 n=0.6233	0.1367 n=0.7546	1.205	1.626
γ-MnO_2/MCMB-catalyzed	0.8166e-6	0.505	0.201	0.8252e-3 n=0.8404	0.2285e-1 n=0.8093	0.092	0.1322

resistance (R_1) is very small for two air electrodes, whereas ohm resistance addition to interface resistance (R_2) and electrochemical polarization resistance (R_3) are clearly different. Specially, γ-MnO_2/MCMB-catalyzed air electrode has lower values of R_2, R_3 and Z_w than that of the γ-MnO_2-catalyzed air electrode. So, it can evidently conclude that employing γ-MnO_2/MCMB as catalyst can reduce R_2 and R_3, *i.e.*, prepared γ-MnO_2/MCMB is favourable to the oxygen reduction reaction. The reason may be attributed to the high surface area, special surface morphology and high conductivity of the material.

Conclusion

A nanostructured γ-MnO_2/MCMB composite prepared by a wet chemical method was investigated as electrocatalyst for oxygen reduction reaction both in alkaline solution and all solid-state zinc-air cell system. Polarization and discharge tests show that γ-MnO_2/MCMB enhanced electrochemical catalytic activity for the oxygen reduction reaction. Rod-like γ-MnO_2 protrusions and small pore size of γ-MnO_2/MCMB resulted in a small contact resistant, ohm resistant and electrochemical polarization of catalyzed air electrode, which caused γ-MnO_2/MCMB having potential application in zinc-air cells.

ACKNOWLEDGEMENTS

This work was supported by Yangtze Normal University Research Start-up Foundation and Science and Technology Research Project of Chongqing Education Board (KJ081304).

REFERENCES

1. M. Oshitani, M. Watada, K. Shodai and M. Kodama, *J. Electrochem. Soc.*, **148**, A67 (2001).
2. S.I. Pyun and Y.G. Ryu, *J. Power Sources*, **62**, 1 (1996).
3. C.C. Chang, T.C. Wen and H.J. Tien, *Electrochim. Acta*, **42**, 557 (1997).
4. D.B. Zhou and H.V. Poorten, *Electrochim. Acta*, **40**, 1819 (1995).
5. E. Passalacqua, G. Squadrito and F. Lufrano, *J. Appl. Electrochem.*, **31**, 449 (2001).
6. Z. Wei, W. Huang, S. Zhang and J. Tan, *J. Power Sources*, **91**, 83 (2000).
7. R. Othman, W.J. Basirum, A.H. Yahaya and A.K. Arof, *J. Power Sources*, **103**, 34 (2001).
8. Y.L. Cao, H.X. Yang, X.P. Ai and L.F. Xiao, *J. Electroanal. Chem.*, **557**, 127 (2003).
9. A. Restovic, G. Poillerat, P. Chartier and J.L. Gautier, *Electrochim. Acta*, **39**, 1579 (1994).
10. P. Zóltowski, D.M. Dra•ic and L. Vorkapic, *J. Appl. Electrochem.*, **3**, 271 (1973).
11. R.P. Kingsborough and T.M. Swager, *Chem. Mater.*, **12**, 872 (2000).
12. C.J. Chang, Y. Deng, D.G. Nocera, C. Shi, F.C. Anson and C.K. Chang, *Chem. Commun.*, **15**, 1355 (2000).
13. T.D. Chung and F.C. Anson, *J. Electroanal. Chem.*, **508**, 115 (2001).
14. J.P. Brenet, *J. Power Sources*, **4**, 183 (1979).
15. K. Matsuki and H. Kamada, *Electrochim. Acta*, **31**, 13 (1986).
16. H. Honda and Y. Yamada, *J. Japan. Petrol Inst.*, **16**, 392 (1973).
17. Y. Yamada, T. Imamura, H. Kakiyama, H. Honda, S. Oi and K. Fukuda, *Carbon*, **12**, 307 (1974).
18. Y.G. Wang, Y. Korai and I. Mochida, *Carbon*, **37**, 1049 (1999).
19. H. Honda, *Mol. Cryst. Liq. Cryst.*, **94**, 97 (1983).
20. T. Kasuh, D.A. Scott and M. Mori, *Carbon, Newcastle, Extended Abstracts*, **88**, 146 (1988).
21. C.Y. Wang, H. Jiang, P. Li and J.M. Zheng, *New Carbon Mater.*, **15**, 9 (2000).
22. R. Alcántara, F.J.F. Madrigal, P. Lavela, J.L. Tirado, J.M.J. Mateos, C.G. de Salazar, R. Stoyanova and E. Zhecheva, *Carbon*, **38**, 1031 (2000).
23. J. Yamaura, Y. Ozaki, A. Morita and A. Ohta, *J. Power Sources*, **43**, 233 (1993).
24. A. Mabuchi, K. Tokumitsu, H. Fujimoto and T. Kasuh, *J. Electrochem. Soc.*, **142**, 1041 (1995).
25. K. Tokumitsu, H. Fujimoto, A. Mabuchi and T. Kasuh, *Carbon*, **37**, 1599 (1999).
26. C. Iwakura, N. Furukawa, T. Ohnishi, K. Sakamoto, S. Nohara and H. Noue, *Electrochemistry*, **69**, 659 (2001).
27. G.Q. Zhang and X.G. Zhang, *Electrochim. Acta*, **49**, 873 (2004).
28. T.D. Xiao, P.R. Strutt, B.H. Kear, H.M. Chen and D.M. Wang, US, Patent, 6,517,802 B1 (2003).

(*Received*: 1 August 2008; *Accepted*: 25 March 2009) AJC-7373